Pure Appl. Geophys. 169 (2012), 641–658

DOI 10.1007/s00024-011-0335-x

Pure and Applied Geophysics

Lg Body-Wave Magnitude Scaling for the Continental Margin around Korea and Japan

Tae-Kyung Hong[1]

Abstract—Regional body-wave magnitude scalings are essential for quantification of small and moderate-size earthquakes that are observed only up to regional distances. Crustally-guided shear waves, *Lg*, develop stably at regional distances in continental crusts and are minimally influenced by the source radiation patterns. *Lg* body-wave magnitude scalings, $m_b(Lg)$, are widely used for assessment of sizes of regional crustal events. The $m_b(Lg)$ scaling has rarely been tested in continental margins where *Lg* waves are significantly attenuated due to abrupt lateral variation of crustal structures. We test the applicability of $m_b(Lg)$ scaling to the eastern margin of the Eurasian plate around the Korean Peninsula and Japanese islands. Both third-peak and root-mean-square (rms) amplitudes of *Lg* vary significantly according to the crustal structures along raypaths, causing apparent underestimation of $m_b(Lg)$. Implementation of raypath-dependent quality factors (Q) allows accurate estimation of $m_b(Lg)$, retaining the transportability of $m_b(Lg)$ in the continental margin around Korea and Japan. The calibration constants for an rms-amplitude-based $m_b(Lg)$ scaling are not determined to vary by region in the continental margin due to complicated crustal structures. The calibration constants are determined to be distance-dependent. Both the third-peak-amplitude-based and rms-amplitude-based $m_b(Lg)$ scalings yield accurate magnitude estimates when raypath-dependent quality factors are implemented.

1. Introduction

The Korean Peninsula and Japanese islands compose the far-eastern margin of the Eurasian plate. A paleo-rifted backarc region is located between the Korean Peninsula and Japanese islands. This continental margin is encompassed by plate boundaries with high seismicity by active plate convergency. Offshore events occur frequently in oceanic regions around the continental margins. The events are recorded well at dense seismic networks in the Korean Peninsula and Japanese islands. Accurate determination of magnitudes of the regional events is an important task in local seismic-monitoring institutions.

It may be desirable to calculate the moment magnitudes that reflect the energy radiated from events. However, the moment magnitude scalings are difficult to be applicable to small-size events. The *Lg* wave is a crustally-guided shear wave, and is the most dominant phase in regional seismograms for crustal earthquakes. It is known that the *Lg* wave is minimally influenced by the source radiation pattern, allowing azimuth-independent stable measurement of magnitudes (e.g., Shi *et al.*, 2000; Phillips and Stead, 2008). Thus, *Lg* body-wave magnitude scalings, $m_b(Lg)$, are widely used for assessing the sizes of regional crustal events.

The *Lg* wavetrains, however, vary significantly with crustal structures (e.g., Kennett and Furumura, 2001; Hong *et al.*, 2008). In particular, the *Lg* waves are dissipated strongly in thin or undulated crusts due to energy leakage into the mantle (e.g., Knopoff *et al.*, 1979; Kennett, 1986; Zhang and Lay, 1995). The backarc region in the East Sea (Sea of Japan) hinders effective transmission of *Lg* (Hong, 2010). Thus, the magnitudes can be underestimated with $m_b(Lg)$ scalings in regions with laterally varying crustal structures when the *Lg* attenuation is not corrected properly.

The $m_b(Lg)$ scaling has been limitedly applied to regional events around the Korean Peninsula (Hong *et al.*, 2008; Zhao *et al.*, 2008). However, the application conditions for $m_b(Lg)$ scaling in the continental margins were rarely investigated. Further, the potential underestimation with $m_b(Lg)$ scaling for events around continental margins is poorly known despite various studies on the transportability of $m_b(Lg)$ (e.g., Priestley and Patton, 1997; Patton, 2001).

[1] Department of Earth System Sciences, Yonsei University, Shinchon-dong, 134, Seodaemun-gu, Seoul 120-749, South Korea. E-mail: tkhong@yonsei.ac.kr

Birkhäuser

The $m_b(Lg)$ is determined with third-peak amplitudes of Lg waves in conventional scalings (e.g., PATTON, 1988). However, it was reported that a $m_b(Lg)$ scaling based on root-mean-square (rms) Lg amplitudes enables more stable determination of magnitudes (PATTON, 1988; HANSEN *et al.*, 1990; RINGDAL *et al.*, 1992; PRIESTLEY and PATTON, 1997). This rms-amplitude-based $m_b(Lg)$ scaling has not been tested to determine whether it is applicable to events around continental margins. Also, it is unclear whether uniform calibration constants can be applied for rms-amplitude-based $m_b(Lg)$ scalings at different regions.

In this study, we test the transportability of $m_b(Lg)$ scaling in the eastern margin of the Eurasian plate around the the Korean Peninsula and Japanese islands. We also investigate the rms-Lg-amplitude variation with distance, and examine the calibration constants for the rms-amplitude-based $m_b(Lg)$ scalings.

2. *Data and Geology*

The far-eastern Asian region around the Korean Peninsula, the East Sea (Sea of Japan) and Japanese islands composes the eastern margin of the Eurasian plate (Fig. 1). This region has experienced a complex tectonic history including collisions of massif blocks and continental rifting and volcanic activities (e.g., CHOUGH *et al.*, 2000). The East Sea is located between the Korean Peninsula and the Japanese islands. It is known that the East Sea was opened by a continental rifting during the Oligocene to mid-Miocene, separating the Japanese islands from the Eurasian plate.

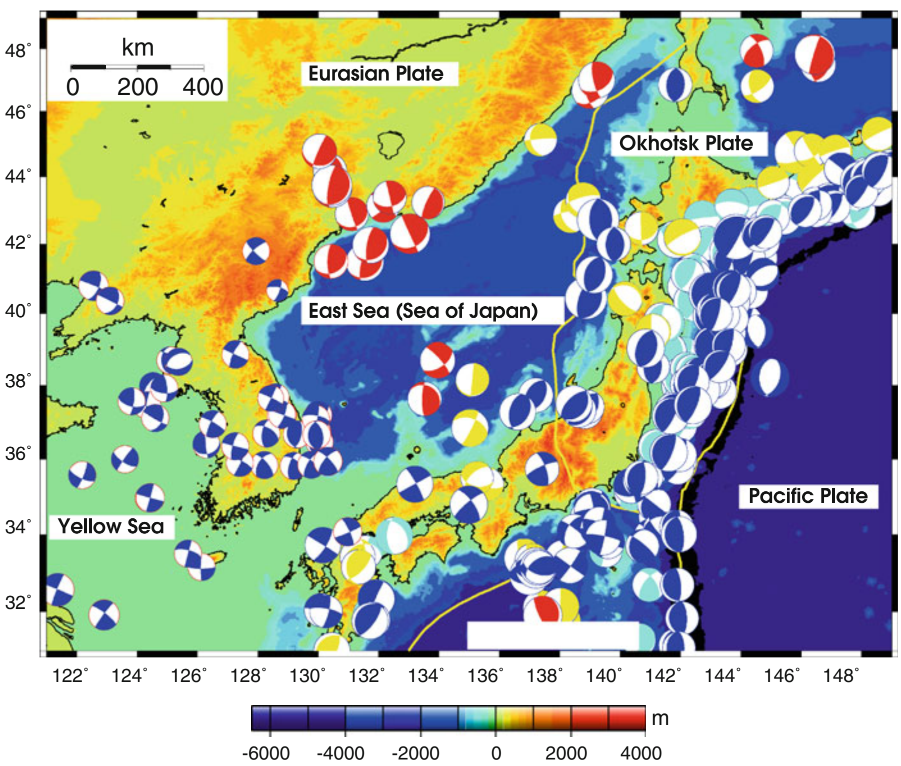

Figure 1
Tectonic structures and focal mechanism of events during 1976–2008 around the Korean Peninsula and Japanese islands are presented. The magnitudes of the events around the Japanese islands are greater than 6, while those around the Korean Peninsula are greater than 3. The colors in focal mechanism solutions indicate the focal depths (*blue*: 0–35 km, *green* 35–100 km, *yellow* 100–400 km, *red* 400–700 km). Shallow seismicity is dominant in the Korean Peninsula, while various depths of earthquakes are observed around the Japanese islands. Shallow thrustal earthquakes frequently occur along the west coast of the Japanese islands

The opening of the East Sea created three backarc basins, the Japan, Yamato and Ulleung basins. The growth of the East Sea was ended in the mid-Miocene by the E–W directional compression of the Pacific plate against the eastern margin of the Eurasian plate (Jolivet and Huchon, 1989). The immature growth of the East Sea caused incomplete development of oceanic crusts in the East Sea. Thus, the crusts in the East Sea display transitional structures from continental to oceanic crusts (Kim *et al*., 2003; Sato *et al*., 2006). This paleo-rifting induced undulation in Moho topography and abrupt lateral variation of crustal structures in the East Sea.

The Pacific and the Philippine Sea plates subduct beneath the Eurasian and the Okhotsk plates, developing long trenches (Japan and Nankai troughs) along the east coast of the Japanese islands (Fig. 1). Various shallow to deep-focus earthquakes occur in the subduction zones. In particular, shallow offshore earthquakes occur frequently around the west coast of the Japanese islands due to shortening of the East Sea by tectonic compression from plate subduction. These shallow events are potential generators of destructive tsunamis in the East Sea, which may cause damage to both the Korean Peninsula and the Japanese islands.

We analyzed regional shallow earthquakes during 2000–2010 that occurred around the Korean Peninsula and Japanese islands (Tables 1, 2). Seismic waveform data with epicentral distances less than 1,500 km were collected from stations in the Korean Peninsula and Japanese islands (Fig. 2). We selected events with focal depths less than 38 km to retrieve fully-developed *Lg* wavetrains. The total number of events analyzed in this study was 120, and the magnitudes were between 2.7 and 7.9.

Typical examples of regional seismograms observed in this region are presented in Fig. 3. The regional seismograms are composed of crustal and mantle-lid phases. The *Lg* waves are crustally-guided shear waves that are developed by multiple reflections in the crust. The regional seismograms display discriminative waveforms that vary significantly with raypaths. The seismograms from continental raypaths display major regional phases clearly (Fig. 3). On the other hand, the seismograms from raypaths across the East Sea show weak *Lg* waves due to abrupt lateral variation of crustal structures (Hong, 2010). We also find that the *Lg* waves from raypaths across the East Sea display longer wavetrains than those from pure continental raypaths (Hong *et al*., 2008).

The study region was divided into two subregions: region A for the Japanese islands, and region B for the Korean Peninsula (Fig. 2). The reference magnitudes and event information were collected from the Japan Meteorological Agency (JMA) for the events in region A (Table 1), and from the Korea Meteorological Agency (KMA) and the Korea Institute of Geoscience and Mineral Resources (KIGAM) for those in region B (Table 2). Magnitude estimates M_{JMA} and Mw were collected from JMA, and M_{L} from KMA and KIGAM. Additional event information was collected from the International Seismological Centre (ISC).

3. Theory and Process

The conventional regional body-wave magnitudes were measured from waveform records on the short-period seismometers of the World-Wide Standardized Seismograph Network (SP-WWSSN) (Nuttli, 1986). The SP-WWSSN records were obtained by convolving the ground motions with the SP-WWSSN instrument response. The *Lg* amplitudes were measured from the SP-WWSSN records in time windows bounded by group velocities of 3.6 and 3.2 km/s (Priestley and Patton, 1997). We examined each *Lg* waveform manually, and excluded the waveform records contaminated by noise. The *Lg* wavetrains with signal-to-noise ratios greater than 2 were analyzed.

The $m_b(Lg)$ based on *Lg* amplitudes on SP-WWSSN was calculated by (Nuttli, 1986; Patton and Schlittenhardt, 2005)

$$m_b(Lg) = 5.0 + \log\left[\frac{A(10)}{C}\right], \qquad (1)$$

where $A(10)$ is the hypothetical *Lg* amplitude in the unit of μm at a distance of 10 km, and C is a region-independent calibration constant that is given by 110 μm for a 1 Hz *Lg* wave (Nuttli, 1986).

The hypothetical *Lg* amplitude at a distance of 10 km, $A(10)$, can be calculated by

Table 1

Source parameters of events around the Japanese islands (region A in Fig. 2)

Date (yyyy/mm/dd)	Time (hh:mm:ss)	Lat (°N)	Lon (°E)	Dep (km)	M_W	M_{JMA}	$m_b(Lg)$ (3rd)	$m_b(Lg)$ (Nuttli)	$m_b(Lg)$ (Patton)
2000/06/06	21:16:41.4	36.8	135.5	2.3	5.8	5.8	5.89	5.88	5.88
2000/07/01	07:01:55.6	34.2	139.2	8.9	6.2	6.1	5.86	5.85	5.86
2000/07/08	18:57:45.1	34.2	139.2	10.0	5.9	6.1	5.57	5.58	5.58
2000/07/15	01:30:31.3	34.3	139.2	13.1	6.0	5.9	5.87	5.87	5.87
2000/07/30	12:25:45.5	33.9	139.4	8.4	6.4	6.2	6.14	6.15	6.14
2000/10/03	04:13:28.6	40.2	143.1	19.3	6.0	5.8	6.23	6.23	6.23
2000/10/06	04:30:17.5	35.4	133.2	0.6	6.6	7.1	6.74	6.74	6.75
2002/02/12	13:44:37.9	36.6	141.0	0.0	5.5	5.5	6.04	6.02	6.02
2002/07/23	20:05:30.9	37.3	142.2	24.8	5.5	5.8	6.24	6.22	6.23
2003/09/25	19:50:07.3	41.7	143.9	33.0	7.9	7.8	7.36	7.41	7.40
2003/09/25	21:07:59.8	41.7	143.6	31.8	7.3	7.0	7.07	7.08	7.08
2003/10/31	01:06:30.6	37.9	142.6	23.0	6.7	6.8	6.62	6.61	6.62
2003/11/01	13:10:07.9	37.8	143.1	10.2	5.7	6.2	5.95	5.96	5.97
2004/06/25	21:42:20.2	40.0	138.6	10.8	4.8	5.0	4.93	4.92	4.93
2004/09/05	10:07:07.2	33.1	136.7	18.7	7.2	6.9	6.64	6.64	6.64
2004/09/05	14:57:28.3	33.2	137.1	1.2	7.5	7.4	6.73	6.74	6.75
2004/09/06	23:29:34.9	33.2	137.3	16.6	6.5	6.4	6.33	6.32	6.32
2004/09/08	14:58:26.0	33.2	137.2	30.4	6.1	6.2	5.81	5.81	5.81
2004/10/23	09:34:05.7	37.3	138.9	23.0	6.3	6.3	6.10	6.11	6.11
2004/10/24	21:04:57.2	37.4	138.8	18.3	5.6	5.6	5.44	5.46	5.46
2004/10/27	01:40:49.7	37.3	139.0	19.9	5.8	6.0	5.80	5.80	5.80
2005/01/19	06:11:32.2	34.0	141.5	12.7	6.5	6.8	6.08	6.08	6.08
2005/01/21	12:45:30.9	34.1	141.6	12.5	5.5	5.8	5.55	5.55	5.56
2005/08/24	10:15:28.2	38.6	143.0	10.0	5.9	6.3	6.03	6.03	6.04
2005/08/30	18:10:45.5	38.5	143.2	21.1	6.0	6.2	6.05	6.04	6.04
2005/10/19	11:44:42.8	36.4	140.8	32.0	6.3	6.3	6.24	6.22	6.22
2005/12/02	13:13:09.5	38.1	142.1	29.0	6.5	6.4	6.40	6.41	6.41
2006/03/27	02:50:26.4	32.7	132.0	22.2	5.5	5.5	5.81	5.80	5.80
2006/10/10	23:58:04.0	37.2	142.7	9.0	5.6	6.0	5.84	5.84	5.84
2007/02/17	00:02:56.0	41.8	143.6	31.0	6.0	6.2	6.30	6.31	6.28
2007/03/25	00:41:57.8	37.3	136.6	8.0	6.7	7.1	6.50	6.50	6.50
2007/04/15	03:19:30.4	34.8	136.2	15.7	5.0	5.3	5.48	5.46	5.46
2007/04/26	00:02:58.0	33.9	133.5	38.0	5.0	5.3	5.46	5.48	5.48

The reported magnitudes (M_W, M_{JMA}) of the Japan Meteorological Administration (JMA) are presented. The *Lg* body-wave magnitude estimates ($m_b(Lg, 3rd)$, $m_b(Lg$, Nuttli), $m_b(Lg$, Patton)) are presented

$$A(10) = A(d) \times \sqrt[3]{\frac{d}{10}} \times \sqrt{\frac{\sin(d/111.1)}{\sin(10/111.1)}} \times \exp[\gamma(d-10)], \quad (2)$$

where d is the epicentral distance in km, $A(d)$ is the third (3rd) largest zero-to-peak *Lg* amplitude on the vertical component. Parameter γ is a frequency-dependent attenuation coefficient:

$$\gamma(f) = \frac{\pi f}{vQ}, \quad (3)$$

where f is the frequency, v is the group velocity, and Q is the quality factor. Regional *Lg* is dominant at frequencies around 1 Hz (Nuttli, 1973; Hong *et al.*, 2008). Thus, quality factors for 1 Hz *Lg* waves (i.e., Q_0) were implemented as reference quality factors in this study.

We considered both constant Q and raypath-dependent Q to examine the influence of crustal structures on $m_b(Lg)$ estimates. The raypath-dependent Q, Q_{adapt}, can be calculated by

$$\frac{1}{Q_{adapt}} = \frac{1}{l} \int_{path} \frac{1}{Q} \, dl, \quad (4)$$

where l is the epicentral distance between source and receiver. The raypath-dependent quality factors were

Table 2

Source parameters of events around the Korean Peninsula (region B in Fig. 2)

Date (yyyy/mm/dd)	Time (hh:mm:ss)	Lat (°N)	Lon (°E)	Dep (km)	M_L (KIGAM)	M_L (KMA)	$m_b(Lg)$ (3rd)	$m_b(Lg)$ (Nuttli)	$m_b(Lg)$ (Patton)
2000/08/05	12:03:00.0	34.6	125.4	5.3	3.4	2.7	3.10	3.05	3.05
2000/08/21	10:43:38.0	38.9	125.8	10.0	3.6	3.4	3.57	3.62	3.61
2000/12/09	09:51:00.0	36.5	130.0	−1.0	3.9	3.7	4.45	4.44	4.44
2001/01/29	02:44:08.6	35.7	126.7	0.8	3.5	3.0	3.64	3.64	3.64
2001/04/03	21:14:43.0	34.0	131.8	0.2	4.0	–	4.13	4.19	4.19
2001/05/05	11:21:17.8	38.3	124.4	10.7	3.5	3.3	3.45	3.39	3.39
2001/07/23	08:29:14.6	36.5	128.0	13.6	3.6	3.5	3.46	3.48	3.48
2001/08/24	02:12:03.5	35.9	128.2	1.7	3.2	3.1	3.16	3.13	3.12
2001/11/21	01:49:11.6	36.7	128.3	0.5	3.6	3.5	3.84	3.86	3.86
2001/11/24	07:10:32.0	36.7	129.9	7.1	4.1	4.1	4.23	4.19	4.19
2002/01/07	08:10:00.2	35.3	128.9	5.0	2.8	3.1	2.82	2.89	2.89
2002/03/07	14:30:57.2	36.4	126.6	0.3	3.2	3.0	3.04	3.05	3.05
2002/03/17	00:26:41.1	38.2	124.5	33.0	3.8	3.9	4.13	4.14	4.14
2002/03/22	02:28:55.2	38.1	124.6	1.3	3.0	3.5	3.13	3.14	3.14
2002/04/16	22:52:38.6	40.7	128.7	10.0	3.4	3.9	4.87	4.96	4.95
2002/07/08	19:01:49.9	35.9	129.8	11.5	3.7	3.8	4.13	4.13	4.13
2002/07/16	21:50:30.7	38.0	125.2	0.8	3.4	3.3	3.38	3.37	3.37
2002/08/05	22:32:39.5	34.7	127.4	7.9	2.8	3.0	2.44	2.46	2.46
2002/09/17	09:08:11.8	36.5	124.0	2.3	3.6	–	3.86	3.86	3.87
2002/10/19	19:22:07.7	35.2	127.7	9.7	2.8	3.0	2.56	2.62	2.61
2002/12/09	22:42:49.8	38.9	127.3	0.7	4.1	3.8	4.15	4.13	4.13
2003/01/09	08:33:21.2	37.5	124.6	5.0	3.9	3.9	4.14	4.12	4.12
2003/03/01	14:33:28.5	35.8	129.4	10.4	3.2	3.0	3.31	3.18	3.18
2003/03/09	18:28:03.2	36.1	128.4	1.2	3.1	3.1	3.22	3.24	3.24
2003/03/22	20:38:40.4	35.0	124.4	10.0	5.1	4.9	5.41	5.42	5.42
2003/04/15	17:55:23.9	36.4	126.2	0.7	3.5	3.3	3.55	3.53	3.53
2003/07/05	03:18:29.9	37.4	125.3	5.0	3.1	3.0	3.19	3.16	3.16
2003/10/13	09:12:04.9	37.0	126.5	5.4	3.9	3.6	4.12	4.12	4.12
2004/01/05	16:49:42.9	38.7	125.1	1.0	3.4	3.2	3.53	3.53	3.53
2004/04/26	04:29:25.0	35.8	128.2	8.2	4.0	3.9	4.11	4.11	4.11
2004/05/05	03:22:27.8	32.4	125.9	0.0	3.0	3.1	3.50	3.47	3.47
2004/05/29	10:14:28.4	36.6	129.9	29.2	5.1	5.2	5.46	5.46	5.46
2004/06/01	11:22:17.7	37.2	130.1	10.2	3.7	3.5	3.85	3.78	3.78
2004/08/05	20:32:53.3	35.9	127.3	0.3	3.6	3.3	3.60	3.57	3.57
2005/02/20	13:18:38.8	35.4	126.2	14.1	3.5	3.4	3.60	3.57	3.57
2005/03/17	14:39:54.8	32.6	126.0	0.0	3.0	3.1	3.55	3.49	3.49
2005/03/20	01:53:41.1	33.8	130.2	9.0	6.5	7.0	6.36	6.36	6.36
2005/03/22	06:55:33.1	33.7	130.2	6.0	–	5.1	4.83	4.84	4.84
2005/03/24	14:38:42.7	33.7	130.2	13.5	–	4.1	3.97	3.98	3.98
2005/03/25	12:03:19.9	33.8	130.1	12.9	3.9	4.3	4.27	4.25	4.26
2005/04/19	21:11:27.0	33.6	130.3	18.8	4.7	5.7	5.36	5.37	5.36
2005/04/20	00:09:43.2	33.7	130.3	20.4	4.6	5.1	5.20	5.19	5.19
2005/04/21	03:37:32.9	34.9	125.4	13.8	3.1	3.0	3.29	3.30	3.31
2005/06/14	22:07:04.2	33.3	126.0	10.0	3.8	3.7	4.26	4.24	4.25
2005/06/14	22:37:50.8	33.3	126.1	0.0	2.9	3.0	3.22	3.18	3.18
2005/06/20	06:31:50.6	38.7	125.8	0.0	2.7	3.0	3.20	3.14	3.14
2005/06/29	14:18:03.8	34.4	129.2	5.5	3.7	4.0	4.14	4.14	4.14
2005/06/29	15:25:02.5	36.7	129.8	6.4	3.1	3.1	3.45	3.47	3.47
2005/07/29	18:01:37.4	34.2	127.5	8.0	3.0	3.1	3.20	3.20	3.21
2005/08/23	20:06:24.5	34.2	127.0	7.7	3.3	3.5	3.73	3.75	3.75
2005/10/09	23:51:08.3	37.8	125.0	4.5	3.6	3.4	3.93	3.89	3.89
2005/10/21	03:00:31.5	37.8	125.0	3.3	3.2	3.0	3.41	3.39	3.39
2005/11/15	00:10:50.6	37.2	128.8	1.8	3.3	3.0	3.52	3.51	3.51
2005/11/27	02:47:09.0	38.2	124.3	19.1	2.8	3.1	3.44	3.43	3.43

Table 2 *continued*

Date (yyyy/mm/dd)	Time (hh:mm:ss)	Lat (°N)	Lon (°E)	Dep (km)	M_L (KIGAM)	M_L (KMA)	$m_b(Lg)$ (3rd)	$m_b(Lg)$ (Nuttli)	$m_b(Lg)$ (Patton)
2006/01/19	03:35:35.5	37.2	128.8	3.1	3.5	3.2	3.90	3.89	3.89
2006/02/13	18:31:48.6	38.9	126.0	10.0	3.2	3.0	3.34	3.39	3.39
2006/04/03	09:14:05.8	38.7	126.0	0.0	3.5	3.3	3.49	3.53	3.53
2006/04/19	00:49:34.3	37.1	129.9	7.6	2.8	3.0	3.35	3.36	3.36
2006/04/28	14:47:55.3	37.1	129.9	12.3	2.9	3.0	3.35	3.36	3.36
2006/04/29	02:01:13.1	37.1	129.9	7.8	3.2	3.5	3.82	3.82	3.82
2006/05/13	10:14:31.5	34.1	129.2	24.9	3.5	–	4.06	4.07	4.07
2006/09/29	14:07:55.5	34.2	125.0	18.9	3.2	3.4	3.52	3.50	3.50
2007/01/20	11:56:53.6	37.7	128.6	13.1	4.9	4.8	5.24	5.22	5.22
2007/09/16	16:16:33.8	36.5	129.6	2.1	3.2	3.0	3.49	3.48	3.48
2007/12/31	21:33:31.1	40.4	127.1	12.5	3.3	3.0	4.30	4.33	4.33
2008/01/16	10:58:01.6	35.6	125.3	12.7	3.9	3.9	4.31	4.29	4.29
2008/02/29	06:53:01.0	38.8	126.2	10.0	2.7	3.2	3.63	3.65	3.64
2008/05/31	12:59:32.6	33.5	125.7	19.8	4.3	4.2	4.70	4.69	4.69
2008/07/23	10:29:57.8	34.5	128.1	14.5	3.2	3.2	3.18	3.16	3.16
2008/09/03	15:44:29.3	35.1	125.0	8.5	2.9	3.0	2.98	2.96	2.96
2008/10/29	00:26:15.5	36.3	127.3	5.7	3.6	3.4	4.10	4.10	4.10
2008/11/11	12:20:54.7	38.5	125.7	13.5	3.4	3.0	3.46	3.46	3.46
2008/11/11	12:30:03.7	38.5	125.7	11.2	3.3	3.0	3.42	3.42	3.42
2008/12/19	08:53:41.9	36.5	129.6	8.4	3.7	3.5	3.91	3.92	3.92
2009/02/15	13:41:58.0	35.7	125.8	18.2	3.2	3.0	2.81	2.98	2.98
2009/03/02	05:20:27.2	37.0	124.7	4.5	3.7	3.4	3.83	3.82	3.82
2009/04/02	11:27:59.1	37.6	125.9	14.6	3.2	3.0	3.22	3.18	3.18
2009/04/29	03:15:42.6	33.4	127.4	7.5	2.7	3.2	2.90	2.90	2.90
2009/05/01	22:58:28.0	36.6	128.7	11.4	3.9	4.0	4.34	4.33	4.33
2009/06/28	13:07:47.6	35.8	128.3	15.3	3.1	3.0	3.10	3.16	3.16
2009/07/14	19:04:49.5	35.1	125.0	6.4	3.5	3.1	3.66	3.69	3.69
2009/08/21	14:02:21.6	38.9	125.8	12.2	3.6	3.8	3.64	3.59	3.60
2010/02/09	09:08:13.7	37.4	126.8	9.5	3.3	3.0	3.39	3.38	3.37
2010/02/16	09:53:31.8	35.6	130.0	18.7	3.6	3.2	3.72	3.73	3.74
2010/02/22	14:29:30.4	33.3	127.2	4.1	3.0	3.0	3.06	3.10	3.10
2010/03/09	03:50:14.1	36.4	125.7	18.0	3.3	3.2	3.27	3.29	3.29

The reported magnitudes of two local institutes (M_L(KIGAM), M_L(KMA)) are presented. The *Lg* body-wave magnitude estimates (m_b(*Lg*, *3rd*), m_b(*Lg*, Nuttli), m_b(*Lg*, Patton)) are presented

calculated based on the *Lg Q* model of Hong (2010) (Fig. 2). Examples of the calculated quality factors along raypaths are presented in Fig. 3. Typical *Lg Q* is observed from continental regions, while low *Lg Q* is observed from oceanic paths. These observed *Lg Q* features are consistent with other studies (e.g., Xie *et al.*, 2006).

It was reported that rms *Lg* amplitudes, $A_{\rm rms}$, are more stable than third-peak *Lg* amplitudes, $A_{\rm 3rd}$ (Patton, 1988; Hansen *et al.*, 1990; Ringdal *et al.*, 1992; Priestley and Patton, 1997). It is expected that $m_b(Lg)$ scalings based on rms amplitudes yield very stable magnitude estimates. However, the rms-amplitude-based $m_b(Lg)$ scalings need to implement calibration constants that should be determined by region to sustain the transportability of magnitude scaling. In this study, we use notations $m_b(Lg, 3{\rm rd})$ and $m_b(Lg, {\rm rms})$ to distinguish between $A_{\rm 3rd}$-based estimates and $A_{\rm rms}$-based estimates.

From Eq. 1, the *Lg* body-wave magnitudes based on rms amplitudes, $m_b(Lg, {\rm rms})$, can be calculated similarly (Patton and Schlittenhardt, 2005):

$$m_b(Lg, {\rm rms}) = 5.0 + \log\left[\frac{A_{\rm rms}(10)}{C_{\rm rms}}\right], \qquad (5)$$

where $C_{\rm rms}$ is a calibration constant for $m_b(Lg, {\rm rms})$. It is known that *Lg* wavetrains are highly influenced by crustal structures (Hong *et al.*, 2008; Hong, 2010). Thus, the amplitude ratios between $A_{\rm rms}$ and $A_{\rm 3rd}$ vary subsequently by region, which requires

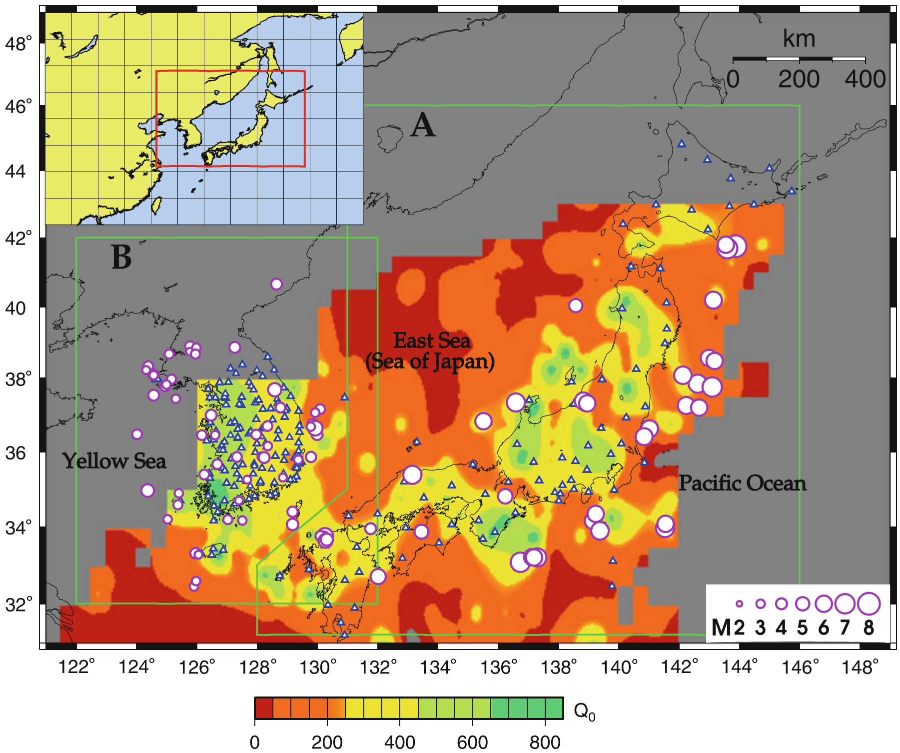

Figure 2
Locations of events (*circles*) and stations (*triangles*) on the Lg quality factor (Q_0) model (Hong, 2010). Low Q_0 is observed in the region around the East Sea, while high Q_0 is found in regions around the Korean Peninsula and Japanese islands. The study region is divided into two sub-regions for comparison: region A for the Japanese islands and region B for the Korean Peninsula

determination of the calibration constant C_{rms} by region.

The hypothetical Lg-rms-amplitude at a distance of 10 km, $A_{rms}(10)$, was calculated by Patton and Schlittenhardt (2005)

$$A_{rms}(10) = A_{rms}(d) \times \left(\frac{d}{10}\right) \times \exp[\gamma(d-10)], \quad \text{for } d \leq 1{,}200\,\text{km},$$
$$= A_{rms}(d) \times \left[\frac{\sin(d/111.1)}{\sin(10/111.1)}\right] \times \exp[\gamma(d-10)], \quad \text{for } d > 1{,}200\,\text{km}, \tag{6}$$

where d is the epicentral distance. Since most waveform data were collected at near regional distances in this study, we determined $A_{rms}(10)$ with the equation for $d \leq 1{,}200$ km in Eq. 6.

To test the validity and stability of rms-amplitude-based $m_b(Lg)$ scalings, we calculated the hypothetical Lg rms amplitudes at a distance of 10 km ($A_{rms}(10)$) from both Eqs. 2 and 6. We denote the hypothetical Lg rms-amplitude based on Eq. 6 as $A_{rms,Patton}(10)$, and that based on Eq. 2 as $A_{rms,Nuttli}(10)$ in this study. Similarly, the calibration constant for $A_{rms,Patton}(10)$ is denoted as $C_{rms,Patton}$, and that for $A_{rms,Nuttli}(10)$ as $C_{rms,Nuttli}$. The Lg body-wave magnitudes based on $C_{rms,Patton}$ are referred to as$m_b(Lg, \text{Patton})$, and those based on $C_{rms,Nuttli}$ as $m_b(Lg, \text{Nuttli})$.

4. *Determination of Calibration Constants for rms Amplitudes*

In principle, the $m_b(Lg)$ scalings based on rms amplitudes should be equivalent to those based on third-peak amplitudes. It is known that a linear relationship holds between peak and rms amplitudes (e.g., Priestley and Patton, 1997). However, Lg waveforms change significantly by crustal structures

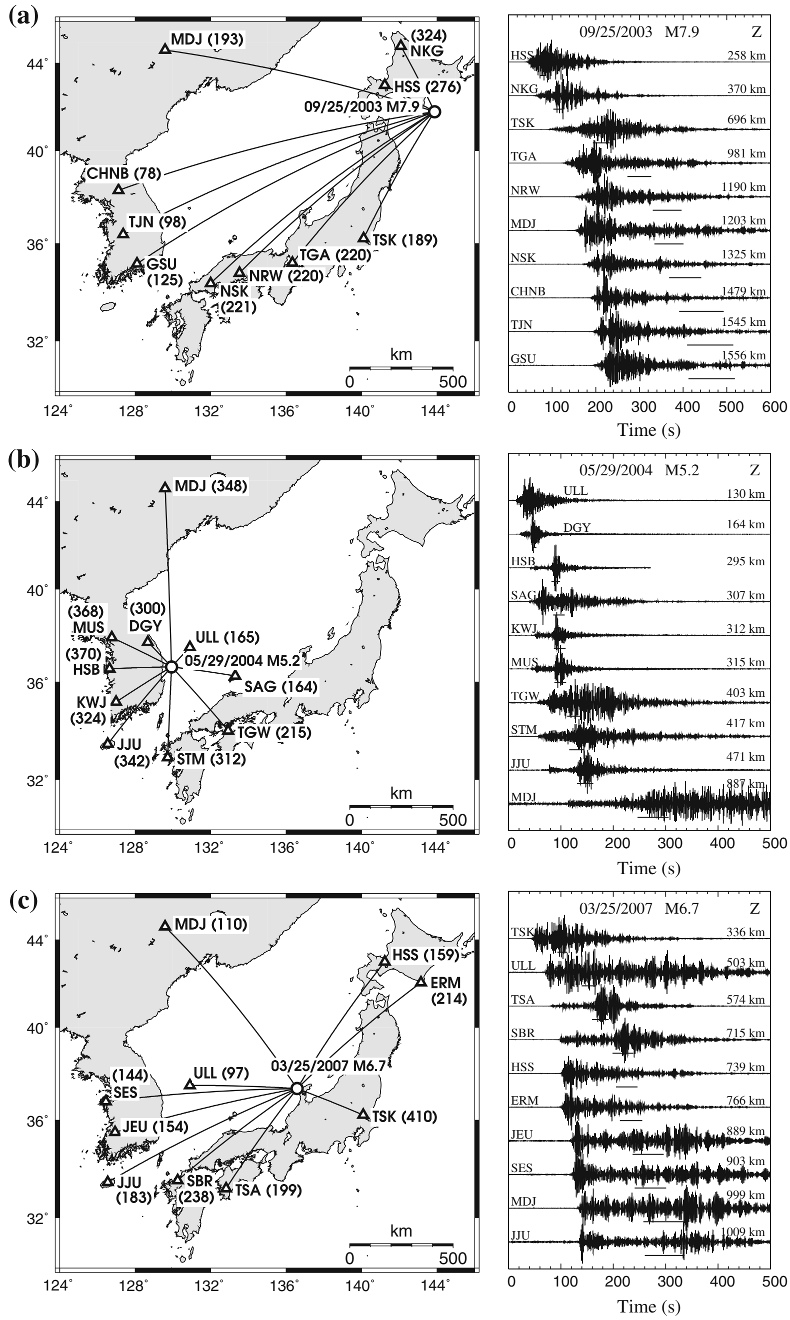

Figure 3

Examples of observed regional seismograms for three crustal events around the Korean Peninsula and the Japanese islands: **a** the 25 September 2003 M7.9 earthquake off the east coast of Hokkaido, **b** the 29 May 2004 M5.2 earthquake off the east coast of the Korean Peninsula, and **c** the 25 March 2007 M6.7 earthquake off the west coast of the Noto Peninsula (central Japan). The great-circle paths are presented with *solid lines*. The *Lg* quality factors (Q_0) along the raypaths are denoted in the *parentheses*. The raypaths across the East Sea have low quality factors. The *Lg* wavetrains are marked with *solid underlines* on the seismograms. The epicentral distances are denoted on the seismograms. The *Lg* waves are highly attenuated along raypaths across the East Sea, but are visible in most raypaths

(Fig. 3). Thus, a single linear relationship is not applicable to regions with complex crustal structures. We determined the calibration constants for rms-amplitude-based $m_b(Lg)$ scalings by regions.

The calibration constants $C_{\mathrm{rms,Nuttli}}$ and $C_{\mathrm{rms,Patton}}$ should be determined so that the magnitude estimates $m_b(Lg, \mathrm{Nuttli})$ and $m_b(Lg, \mathrm{Patton})$ are equal to $m_b(Lg, \mathrm{3rd})$. Thus, from Eqs. 1 and 5, we derived a relationship between the calibration constants:

$$C_{\mathrm{rms},j} = \frac{A_{\mathrm{rms,j}}(10)}{A_{\mathrm{3rd}}(10)} \times C_{\mathrm{3rd}}, \quad (j = \mathrm{Patton}, \mathrm{Nuttli}), \tag{7}$$

where C_{3rd} is the calibration constant for third-peak-amplitude-based magnitude scaling that is given by 110 µm for 1 Hz Lg waves (Nuttli, 1986).

The amplitude ratios $A_{\mathrm{rms},j}(10)/A_{\mathrm{3rd}}(10)$ can be presented as function of distance from Eqs. 2 and 6. We calculated the calibration constants $C_{\mathrm{rms,Nuttli}}$ and $C_{\mathrm{rms,Patton}}$ from Eq. 7 for two regions around the Japanese islands and the Korean Peninsula (Fig. 4). The calculated $C_{\mathrm{rms,Nuttli}}$ and $C_{\mathrm{rms,Patton}}$ displayed linear variations with distance. The representative variations of $C_{\mathrm{rms,Nuttli}}$ and $C_{\mathrm{rms,Patton}}$ were determined with linear regressions.

We analyzed the seismic waveform data with distances greater than 150 km, in which Lg waves develop stably. Outliers deviated from the mean values by 42% or greater were removed in the linear regressions (Fig. 4). For determination of the calibration constants for the Japanese islands, data from 2,749 of 2,961 waveform records were analyzed. Also, we analyzed data from 2,415 of 3,217 waveform records for determination of calibration constants for the Korean Peninsula.

The calibration constants $C_{\mathrm{rms,Nuttli}}$ and $C_{\mathrm{rms,Patton}}$ for the Japanese islands were determined to be (Fig. 4a)

$$\begin{aligned} C_{\mathrm{rms,Nuttli}} &= 53.53 - 0.0074d, \\ C_{\mathrm{rms,Patton}} &= 89.90 + 0.0075d, \end{aligned} \tag{8}$$

where d is the epicentral distance in kilometers. From Eq. 8, the $C_{\mathrm{rms,Patton}}$ was determined to be 91.0 for $d = 150$ km, 95.5 for $d = 750$ km, and 101.2 for $d = 1{,}500$ km. On the other hand, $C_{\mathrm{rms,Nuttli}}$ was determined to be 52.4 for $d = 150$ km, 48.0 for $d = 750$ km, and 42.4 for $d = 1{,}500$ km.

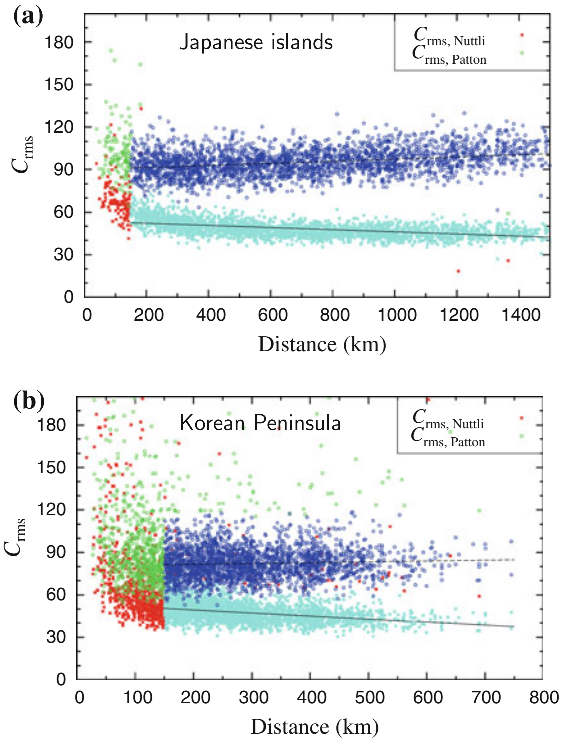

Figure 4
Variation of the calibration constants for root-mean-square (rms) Lg amplitudes ($C_{\mathrm{rms,Nuttli}}$, $C_{\mathrm{rms,Patton}}$): **a** region around the Japanese islands and **b** region around the Korean Peninsula. The Lg amplitudes at distances greater than 150 km are analyzed for the determination of calibration constants. Outliers deviated from the mean value by 0.42 times the mean value were excluded in the analysis. The representative calibration constant functions were determined using linear regressions

Similarly, the calibration constants $C_{\mathrm{rms,Nuttli}}$ and $C_{\mathrm{rms,Patton}}$ for the Korean Peninsula were determined to be (Fig. 4b)

$$\begin{aligned} C_{\mathrm{rms,Nuttli}} &= 53.62 - 0.0215d, \\ C_{\mathrm{rms,Patton}} &= 80.48 + 0.0057d. \end{aligned} \tag{9}$$

Here, $C_{\mathrm{rms,Patton}}$ was determined to be 81.3 for $d = 150$ km and 84.8 for $d = 750$ km. On the other hand, $C_{\mathrm{rms,Nuttli}}$ was determined to be 50.4 for $d = 150$ km and 37.5 for $d = 750$ km. The levels of $C_{\mathrm{rms,Nuttli}}$ and $C_{\mathrm{rms,Patton}}$ for the Korean Peninsula were observed to be slightly lower than those for the Japanese islands. This observation suggests that the Lg rms amplitudes develop weakly around the Korean Peninsula relative to those around the Japanese islands.

From Eqs. 8 and 9, the calibration constants $C_{\mathrm{rms,Nuttli}}$ and $C_{\mathrm{rms,Patton}}$ were determined to be weakly distance-dependent in both the Korean Peninsula and Japanese islands. The distance-dependent variations of $C_{\mathrm{rms,Nuttli}}$ and $C_{\mathrm{rms,Patton}}$ may be caused due to discrepancies between actual and theoretical *Lg* geometrical-spreading effects (e.g., Yang, 2002). Note that this observation is not consistent with Patton and Schlittenhardt (2005), who proposed to implement a distance-independent calibration constant $(C_{\mathrm{rms,Patton}})$ of 90 μm for central Europe. Considering the high variations of *Lg* wavetrains in continental margins, it appears to be desirable to implement distance-dependent calibration coefficients for correct estimation of magnitudes from rms amplitudes.

5. *Application to Events around the Japanese Islands*

We applied three *Lg* body-wave magnitude scalings $(m_b(Lg, 3\mathrm{rd}), m_b(Lg, \mathrm{Nuttli}), m_b(Lg, \mathrm{Patton}))$ to shallow events around the Japanese islands. The magnitudes were determined with not only the average (constant) quality factor but also with raypath-dependent quality factors. The average quality factor of 1 Hz *Lg* waves (Q_0) in the regions around the Korean Peninsula and Japanese islands was determined to be 498 (Hong, 2010). The *Lg* body-wave magnitude estimates based on the average Q_0 are presented in Fig. 5.

The magnitude estimates were compared with the reported magnitudes $(M_W, M_{\mathrm{JMA}}))$ of the Japan Meteorological Agency (JMA) (Table 1). We observe systematic differences among the magnitude estimates. The magnitude estimates based on rms amplitudes $(m_b(Lg, \mathrm{Nuttli}), m_b(Lg, \mathrm{Patton}))$ are determined to be slightly larger than those based on third-peak amplitudes $(m_b(Lg, 3\mathrm{rd})))$. In addition, $m_b(Lg, \mathrm{Nuttli})$ were determined to be larger than $m_b(Lg, \mathrm{Patton})$. This feature may be caused due to development of longer *Lg* wavetrains in regions with transitional crustal structures.

The magnitude differences between the magnitude estimates $(m_b(Lg, 3\mathrm{rd}) - m_b(Lg, \mathrm{Nuttli}), m_b(Lg, 3\mathrm{rd}) - m_b(Lg, \mathrm{Patton}), m_b(Lg, \mathrm{Nuttli}) - m_b(Lg, \mathrm{Patton}))$ were determined to be between −0.2 and 0.2 magnitude unit

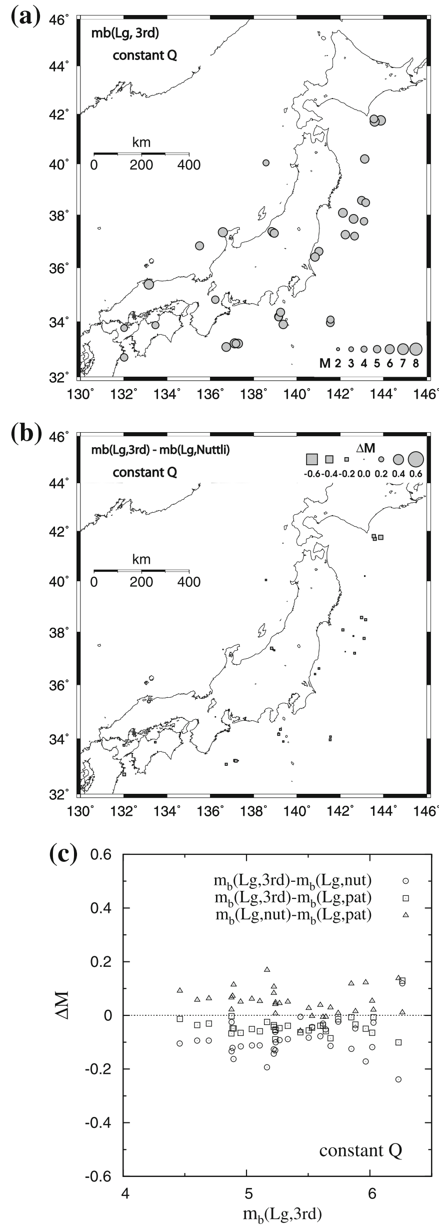

Figure 5

a *Lg* body-wave magnitude estimates based on third-peak amplitudes ($m_b(Lg$, 3rd)) for events around the Japanese islands with implementation of a constant (average) quality factor, **b** differences between magnitude estimates of $m_b(Lg$, 3rd) and $m_b(Lg$, Nuttli), and **c** differences (ΔM) between three magnitude estimates ($m_b(Lg$, 3rd), $m_b(Lg$, Nuttli), $m_b(Lg$, Patton)) as function of $m_b(Lg$, 3rd). Three different magnitude estimates were determined similarly, resulting in magnitude differences distributed in a range between −0.2 and 0.2 magnitude units. The rms-amplitude-based magnitude estimates were determined to be slightly larger than the third-peak-amplitude-based magnitude estimates (i.e., $m_b(Lg$, Nuttli) > $m_b(Lg$, Patton)$m_b(Lg$, 3rd))

(Fig. 5c). We found that the Lg body-wave magnitude estimates based on the average (constant) Q_0 were determined to be lower than the reference magnitudes by ~ 0.7 (Figs. 6, 7). The magnitude differences with respect to the reference magnitudes suggest that the Lg body-wave magnitudes can be underestimated when an average quality factor is applied. This feature may be caused due to higher attenuation of Lg in oceanic regions where crustal structures change abruptly.

We now consider raypath-dependent Q based on a regional Lg Q model (Hong, 2010). The Lg body-wave magnitude estimates based on the raypath-dependent Q are presented in Fig. 8. The magnitude estimates $(m_b(Lg, \text{3rd}), m_b(Lg, \text{Nuttli}), m_b(Lg, \text{Patton}))$ were determined to be similar each other (Fig. 8b, c), which is different from the features observed in the magnitude estimates based on the average (constant) quality factor. We find that the magnitude estimates based on raypath-dependent quality factors were determined to be larger than those based on an average quality factor.

The magnitude estimates based on raypath-dependent quality factors were found to be close to the reference magnitudes, especially for inland events (Figs. 9, 10). This observation suggests that the implementation of raypath-dependent quality factors allows correct estimation of magnitudes. However, some differences were observed between the magnitude estimates and reference magnitudes for large offshore events with magnitudes of $M > 7$ in subduction zones (Fig. 9), which may be due to inherent saturation of body-wave magnitudes for large events (Lay and Wallace, 1995).

6. Application to Events around the Korean Peninsula

Korean local institutes (KIGAM, KMA) report event magnitudes in local magnitude scales (M_L). The local magnitude scalings are applicable to events in local to near regional distances (Ebel, 1982; Kanamori *et al.*, 1993; Kim, 1998). It was reported that M_L estimates are nearly equivalent to m_b estimates (e.g., Herrmann and Nuttli, 1982; Kim, 1998). However, the M_L scalings were applied with assumption that the crustal structures and raypath effects are

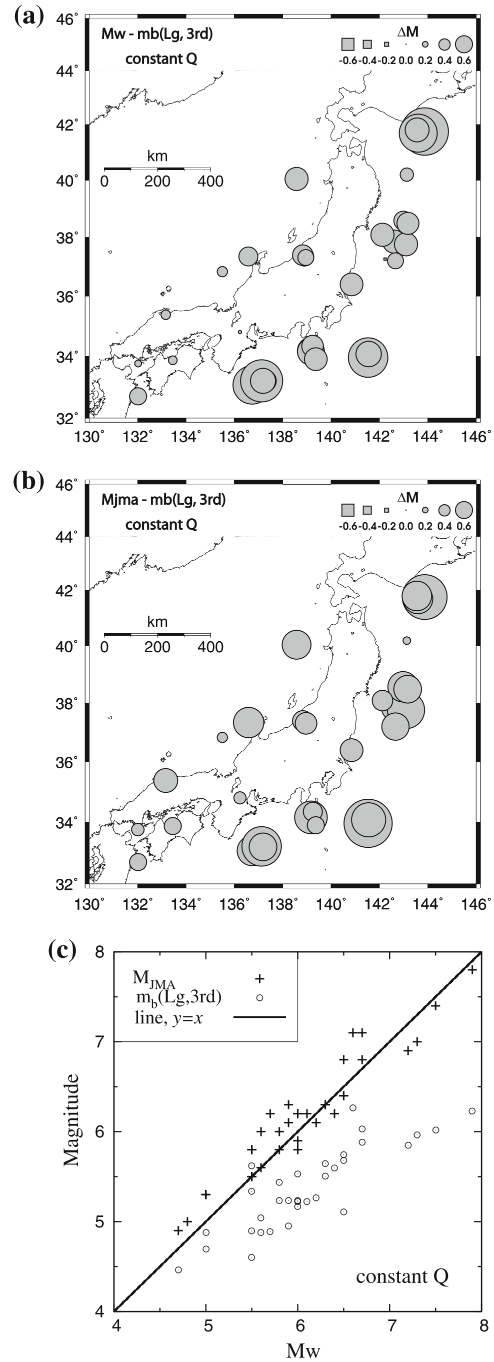

Figure 6
Differences between the reference magnitudes and $m_b(Lg$, 3rd) estimates based on a constant (average) Q for events around the Japanese islands: **a** differences to M_W, **b** differences to M_{JMA}, and **c** comparisons between $M_W - M_{\text{JMA}}$ and $M_W - m_b(Lg$, 3rd). Two reference magnitudes (M_{JMA}, M_W) are similar. The $m_b(Lg$, 3rd) estimates based on an average Q are observed to be much lower than the reference magnitudes

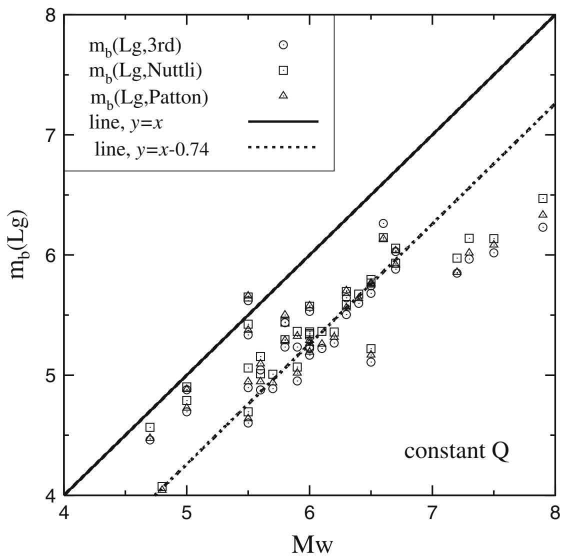

Figure 7
Comparisons among magnitude estimates ($m_b(Lg$, 3rd), $m_b(Lg$, Nuttli), $m_b(Lg$, Patton)) based on a constant (average) Q for events around the Japanese islands. The magnitude estimates are presented as function of reference M_W. The magnitude estimates ($m_b(Lg$, 3rd), $m_b(Lg$, Nuttli), $m_b(Lg$, Patton)) were determined to be similar each other. The magnitude estimates were determined to be lower than the reference M_W by $\sim$0.74 magnitude unit on average

homogeneous. However, the crustal structures change abruptly around the Korean Peninsula, causing significant attenuation of seismic waves (Hong *et al.*, 2008; Hong and Kang, 2009; Hong, 2010). The complex crustal structures around continental margins hinder application of M_L scalings to near-regional events.

The Lg body-wave magnitudes of events around the Korean Peninsula were estimated with implementation of an average (constant) quality factor (Table 2; Fig. 11). The magnitude estimates $(m_b(Lg, 3\text{rd}), m_b(Lg, \text{Nuttli}), m_b(Lg, \text{Patton}))$ were determined to be close (Fig. 11b). The magnitude differences (ΔM) between the magnitude estimates ranged between -0.1 and 0.1 magnitude unit (Fig. 11c).

The Lg body-wave magnitude estimates are compared with the reported M_L of local institutes (Fig. 12). We found that the Lg body-wave magnitude estimates are close to the M_L values for most inland events. However, the Lg body-wave magnitude estimates for offshore and North Korean events were determined to be slightly larger than the M_L

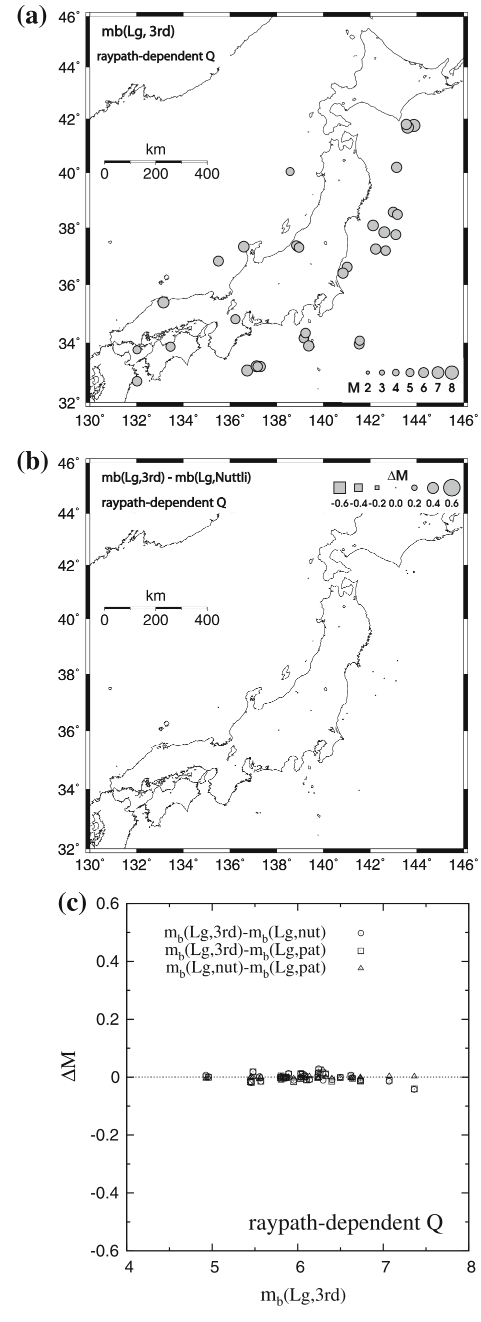

Figure 8
a Lg body-wave magnitude estimates based on third-peak amplitudes ($m_b(Lg$, 3rd)) for events around the Japanese islands with implementation of raypath-dependent Q, **b** differences between magnitude estimates of $m_b(Lg$, 3rd) and $m_b(Lg$, Nuttli), and **c** differences (ΔM) between magnitude estimates($m_b(Lg$, 3rd), $m_b(Lg$, Nuttli), $m_b(Lg$, Patton)) as function of $m_b(Lg$, 3rd). Three different magnitude estimates are determined to be similar to each other. The magnitude differences were found to be much reduced compared to those with an average Q in Fig. 5

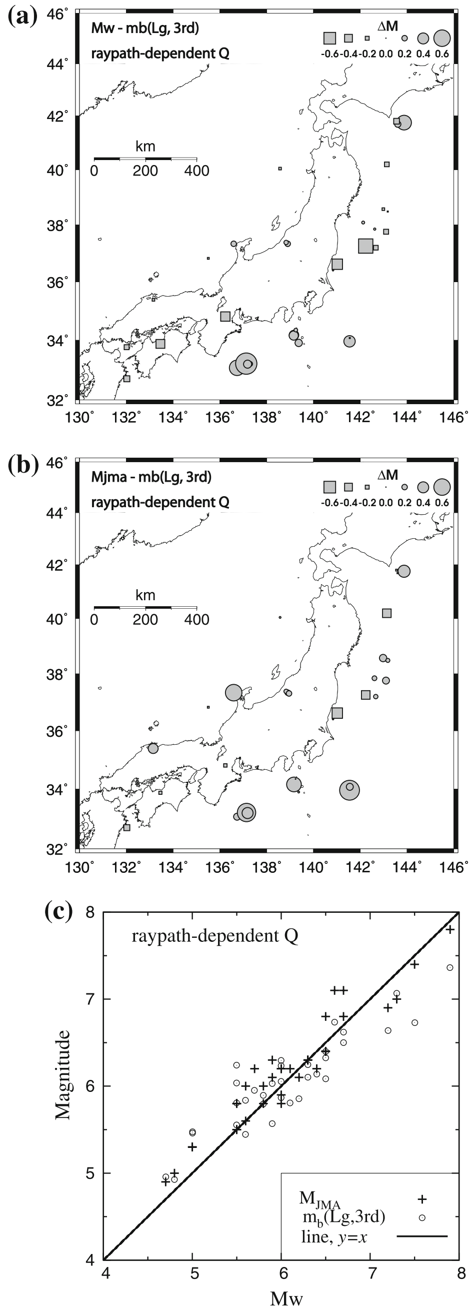

Figure 9
Differences between the m_b(Lg, 3rd) estimates based on raypath-dependent Q and reference magnitudes for events around the Japanese islands: **a** differences to M_W, **b** differences to M_{JMA}, and **c** comparisons between $M_W - M_{\mathrm{JMA}}$ and $M_W - m_b$(Lg, 3rd). Two reference magnitudes (M_{JMA}, M_W) were observed to be similar each other. The m_b(Lg, 3rd) estimates based on raypath-dependent Q were determined close to the reference magnitudes. The events off the east coast of the Japanese islands show relatively large magnitude differences

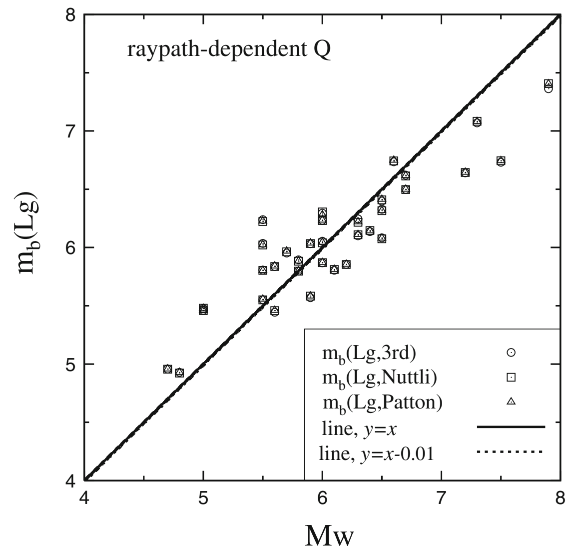

Figure 10
Comparisons among magnitude estimates (m_b(Lg, 3rd), m_b(Lg, *Nuttli*), m_b(Lg, Patton)) based on raypath-dependent Q for events around the Japanese islands. The magnitude estimates are presented as function of reported M_W. The magnitude estimates (m_b(Lg, 3rd), m_b(Lg, Nuttli), m_b(Lg, Patton)) were determined to be similar to the reference M_W. The average magnitude difference was −0.01 magnitude unit

values by 0.13 magnitude unit, on average (Fig. 13). This may be because crustal structures are not homogeneous over large distances and M_L scalings underestimate the event sizes.

We now apply raypath-dependent Q for estimation of the Lg body-wave magnitudes of Korean events. The magnitude estimates $(m_b(Lg, 3\mathrm{rd}), m_b(Lg, \mathrm{Nuttli}), m_b(Lg, \mathrm{Patton}))$ are determined to be similar (Fig. 14). The magnitude estimates based on the raypath-dependent Q were observed to be close to those based on the average (constant) Q for most inland events (Fig. 15). However, we observed increases in magnitude estimates for offshore events when we applied raypath-dependent Q (cf., Fig. 12). This is because the Lg attenuation in the offshore regions is much stronger than the Lg attenuation in the inland regions.

We found that the overall Lg body-wave magnitude estimates based on raypath-dependent Q are larger than the M_L values by $\sim$0.2 magnitude unit (Fig. 16). This magnitude analysis suggests that the magnitudes of offshore events around the Korean Peninsula can be underestimated in the M_L scalings.

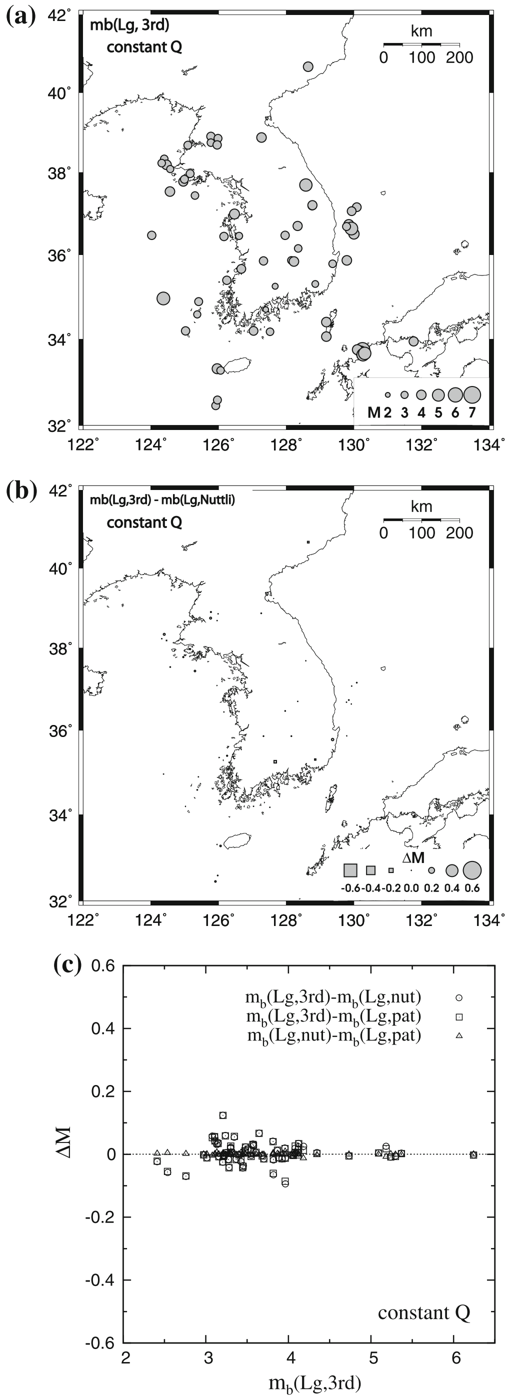

Figure 11

a $m_b(Lg$, 3rd) estimates of events around the Korean Peninsula with implementation of a constant (average) Q, **b** differences between magnitude estimates of $m_b(Lg$, 3rd) and $m_b(Lg$, Nuttli), and **c** differences (ΔM) between various magnitude estimates as function of $m_b(Lg$, 3rd). Three different magnitude estimates were determined to be similar, making the magnitude differences distributed in a range between -0.1 and 0.1 magnitude unit

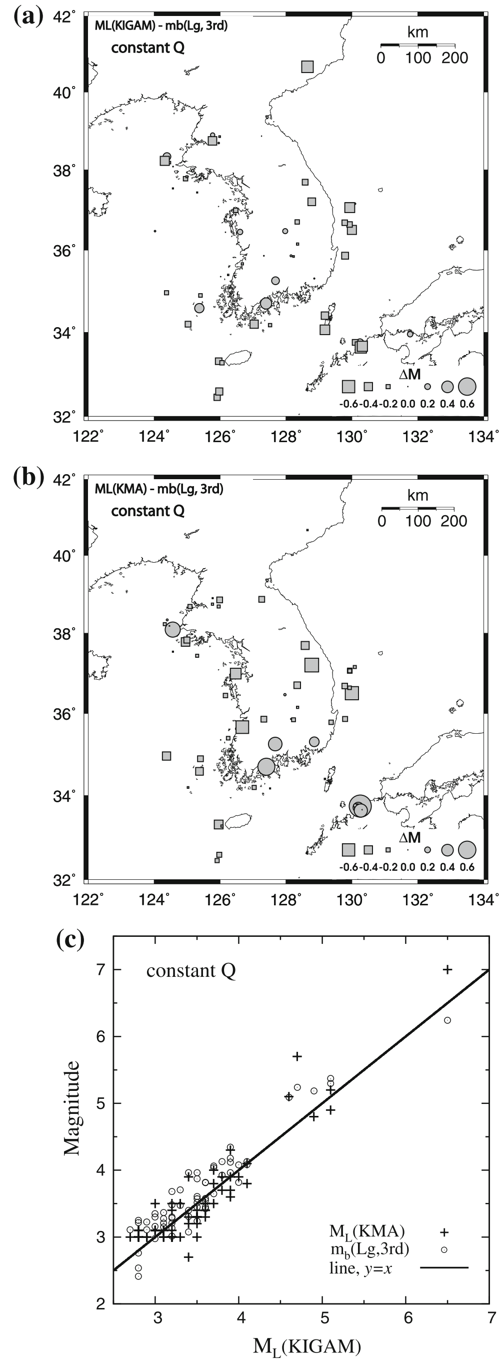

Figure 12

Differences between the reference magnitudes and $m_b(Lg$, 3rd) estimates based on a constant (average) Q for events around the Korean Peninsula: **a** differences to M_L(KIGAM), **b** differences to M_L(KMA), and **c** comparisons between pairs of M_L(KIGAM)-M_L(KMA) and M_L(KIGAM)-$m_b(Lg$, 3rd). M_L(KMA) is close to M_L(KIGAM). The $m_b(Lg$, 3rd) estimates based on an average Q are slightly larger than M_L(KIGAM) values

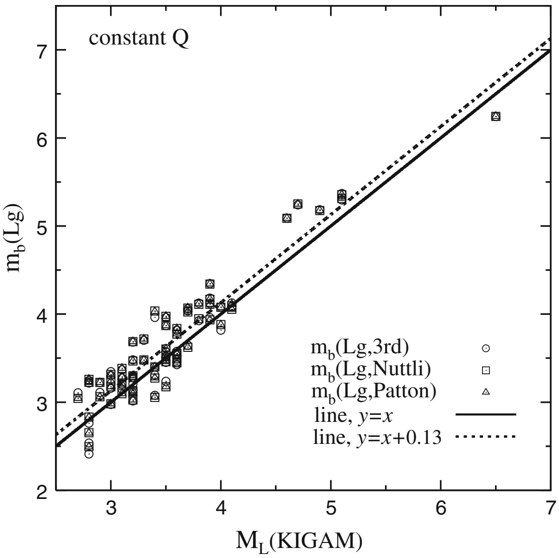

Figure 13
Comparison among magnitude estimates ($m_b(Lg$, 3rd), $m_b(Lg$, Nuttli), $m_b(Lg$, Patton)) based on a constant (average) Q for events around the Korean Peninsula. The reference magnitudes (M_L(KIGAM)) are presented in the horizontal axis. The magnitude estimates ($m_b(Lg$, 3rd), $m_b(Lg$, Nuttli), $m_b(Lg$, Patton)) are determined similar each other. The magnitude estimates are determined to be larger than the reference M_L(KIGAM) by ~ 0.13 magnitude unit on average

Thus, it is desirable to use regional body-wave magnitude scalings in the regions with complex crustal structures instead of local-magnitude scalings.

7. Discussion and Conclusions

Crustally-guided shear waves, *Lg*, are widely analyzed for estimation of magnitudes of regional crustal events because they develop stably in regional distances with minimal influence by the source radiation patterns. Earthquakes occur often in offshore regions around continental margins, in which the *Lg* waves attenuate strongly during propagation due to complex crustal structures. The high variation of *Lg* wavetrains by raypath causes large fluctuation of *Lg* amplitudes, which may cause difficulty in accurate estimation of magnitudes based on *Lg* waves.

The applicability of *Lg* body-wave magnitude scalings to continental margins has rarely been examined. In this study, we tested the applicability of the *Lg* body-wave magnitude scalings in the eastern

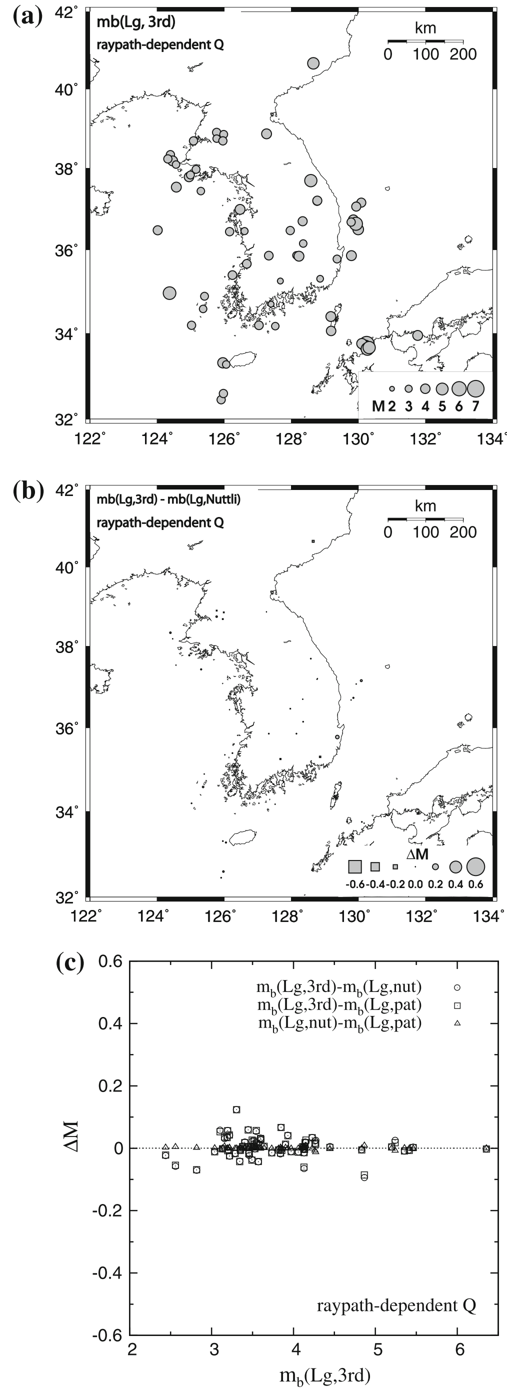

Figure 14
a $m_b(Lg$, *3rd*) estimates of events around the Korean Peninsula with implementation of raypath-dependent Q, **b** difference between magnitude estimates of $m_b(Lg$, 3rd) and $m_b(Lg$, Nuttli), and **c** differences (ΔM) between three magnitude estimates as functions of $m_b(Lg$, 3rd). Three different magnitude estimates are determined to be similar to each other

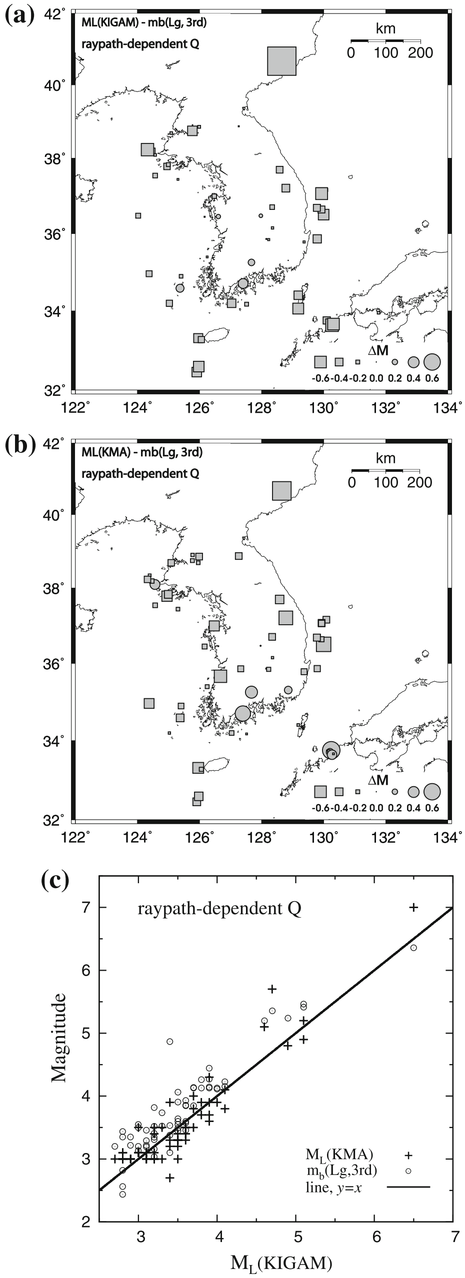

Figure 15

Differences between the reference magnitudes and m_b(*Lg*, 3rd) estimates based on raypath-dependent *Q* for events around the Korean Peninsula: **a** differences to M_L(KIGAM), **b** differences to M_L(KMA), and **c** comparisons between M_L(KIGAM)-M_L(KMA) and M_L(KIGAM)-m_b(*Lg*, 3rd). The reference magnitudes (M_L(KMA), M_L(KIGAM)) are similar to each other. The m_b(*Lg*, 3rd) estimates for earthquakes off the coasts of the Korean Peninsula were determined to be larger than the reference magnitudes, while those for inland events were estimated close to the reference magnitudes

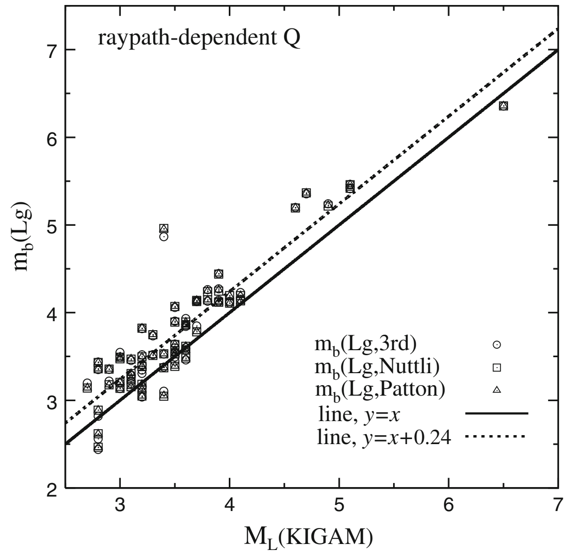

Figure 16

Comparison among magnitude estimates (m_b(*Lg*, 3rd), m_b(*Lg*, *Nuttli*), m_b(*Lg*, Patton)) based on raypath-dependent *Q* for events around the Korean Peninsula. The reference magnitudes (M_L(KIGAM)) are presented. The magnitude estimates (m_b(*Lg*, 3rd), m_b(*Lg*, Nuttli), m_b(*Lg*, Patton)) are determined to be similar to each other. The magnitude estimates were determined to be higher than the reference M_W by 0.24 magnitude unit on average

continental margin of the Eurasian plate where crustal structures change abruptly. We considered raypath-dependent quality factors (*Q*) to recover the *Lg* amplitude correctly. We compared the *Lg* body-wave magnitude estimates based on raypath-dependent quality factors, not only with those based on an average (constant) quality factor, but also with the magnitudes reported by local institutes. We found that the magnitude estimation based on raypath-dependent *Q* enables us to determine correct magnitudes with *Lg* waves.

We also examined the transportability of *Lg* body-wave magnitude scaling based on rms amplitudes at the continental margin. It was found that a distance-dependent correction is required for *Lg* rms amplitudes to be assessed for correct measurement of magnitudes. In addition, it was found that the calibration constant functions for rms amplitudes vary by region. The *Lg* body-wave magnitude estimates based on rms amplitudes $(m_b(Lg, \text{Nuttli}), m_b(Lg, \text{Patton}))$ were determined to be similar to those based on third-peak amplitudes $(m_b(Lg, 3\text{rd}))$. This observation suggests that a linear relationship is held between rms and third-peak amplitudes. Thus, it appears that both rms and third-peak amplitudes with proper correction for attenuations along raypaths can be applicable for assessment of event sizes.

For inland events, the *Lg* body-wave magnitude estimates ($m_b(Lg, 3\text{rd}), m_b(Lg, \text{Nuttli}), m_b(Lg, \text{Patton})$) were determined to be close to the magnitudes reported by local institutes. On the other hand, *Lg* body-wave magnitude estimates were observed to be larger than the reported M_L values for offshore events around the Korean Peninsula. This observation suggests that the magnitudes of offshore events can be underestimated under local-magnitude scalings due to insufficient correction of attenuation. On the other hand, the *Lg* body-wave magnitude scalings based on raypath-dependent quality factors yielded accurate magnitudes consistently for both inland and offshore events. Thus, it was found that the *Lg* body-wave magnitude scalings with implementation of raypath-dependent *Q* can yield accurate magnitude estimates for events in continental margins and backarc regions. Also, both third-peak-amplitude-based and rms-amplitude-based magnitude scalings allow stable estimation of magnitudes.

Careful examination of *Lg* wavetrains, however, is needed to determine correct magnitudes under the *Lg* body-wave magnitude scalings because the *Lg* waves can be weaker than the ambient noise due to attenuation during long propagation in backarc regions. The *Lg* body-wave magnitudes can be overestimated when the noise-contaminated *Lg* waves are analyzed. The *Q*-corrected amplitudes of the noise-contaminated *Lg* waves were observed to be outliers among data sets, and should be excluded in the analysis. When the *Lg* body-wave magnitude scalings are not applicable due to high attenuation, *Pn* body-wave magnitude scalings may be alternatives, because *Pn* waves are less affected by the crustal structures than the *Lg* (e.g., Evernden, 1967; Vergino and Mensing, 1990; Priestley and Patton, 1997).

Acknowledgments

We are grateful to the Korea Meteorological Administration (KMA), the Korea Institute of Geoscience and Mineral Resources (KIGAM), the Incorporated Research Institutions for Seismology (IRIS) and the National Research Institute for Earth Science and Disaster Prevention (NIED) in Japan for making seismic data available. We thank four anonymous reviewers and Professor Brian Mitchell for fruitful review comments. This work was supported by the Korea Meteorological Administration Research and Development Program under Grant CATER 2007-5111.

References

Chough, S.K., Kwon, S.-T., Ree, J.-H., and Choi, D.K., (2000) *Tectonic and sedimentary evolution of the Korean peninsula: a review and new view*, Earth-Science Reviews, *52*, 175-235.

Ebel, J.E., (1982), *$M_{\{L}$ measurements for northeastern United States earthquakes*, Bull Seism. Soc. Am., *72* (4), 1367-1378.

Evernden, J.F., (1967), *Magnitude determination at regional and near-regional distances in the United States*, Bull. Seism. Soc. Am., *57*, 591-639.

Hansen, R.-A., Ringdal, F., and Richards, P.G., (1990), *The stability of RMS Lg measurements and their potential for accurate estimation of the yields of Soviet underground nuclear explosions*, Bull. Seism. Soc. Am., *80* (6B), 2106-2126.

Herrmann, R.B., and Nuttli, O.W., (1982), *Magnitude: the relation of M_L to m_{bLg}*, Bull. Seism. Soc. Am., *72* (2), 389-397.

Hong, T.-K., (2010), *Lg attenuation in a region with both continental and oceanic environments*, Bull. Seism. Soc. Am., *100*, 851-858.

Hong, T.-K., Baag, C.-E., Choi, H., and Sheen, D.-H., (2008). *Regional seismic observations of the October 9, 2006 underground nuclear explosion in North Korea and the influence of crustal structure on regional phases*, J. Geophys. Res., *113*, B03305, doi:10.1029/2007JB004950.

Hong, T.-K., and Kang, T.-S., (2009), *Pn traveltime tomography of the paleo-continental-collision and rifting zone around Korea and Japan*, Bull. Seism. Soc. Am., *99* (1), 416-421.

Jolivet, L., and Huchon, P., (1989), *Crustal scale strike-slip deformation in Hokkaido, Northeast Japan*, Struct. Geol., *11*, 509-522.

Kanamori, H., Mori, J., Hauksson, E., Heaton, T.H., Hutton, L.K., and Jones, L.M., (1993), *Determination of earthquake energy release and M_L using TERRAscope*, Bull. Seism. Soc. Am., *83* (2), 330-346.

Kennett, B.L.N., (1986), *Lg waves and structural boundaries*, Bull. seism. Soc. Am., *76*, 1133-1141.

Kennett, B.L.N., and Furumura, T., (2001), *Regional phases in continental and oceanic environments*, Geophys. J. Int., *146* (2), 562-568.

Kim, H.-J., Jou, H.-T., Cho, H.-M., Bijwaard, H., Sato, T., Hong, J.-K., Yoo, H.-S., and Baag, C.-E., (2003), *Crustal structure of the continental margin of Korea in the East Sea (Japan Sea) from deep seismic sounding data: evidence for rifting affected by the hotter than normal mantle*, Tectonophysics, *364*, 25-42.

Kim, W.-Y., (1998), *The M_L scale in eastern north America*, Bull. Seism. Soc. Am., *88* (4), 935-951.

Knopoff, L., Mitchel, R.G., Kausel, E.G., and Schwab, F., (1979), *A search for the oceanic Lg phase*, Geophys. J. R. Astr. Soc., *56*, 211-218.

LAY, T., and WALLACE, T.C., Modern Global Seismology (Academic Press, Inc., San Diego, CA, 1995).

NUTTLI, O.W., (1973), *Seismic wave attenuation and magnitude relations for eastern North America*, J. Geophys. Res., *78*, 876-885.

NUTTLI, O.W., (1986), *Yield estimates of Nevada test site explosions obtained from seismic Lg waves*, J. Geophys. Res., *91*, 2137-2151.

PATTON, H.J., (1988), *Application of nuttli's method to estimate yield of Nevada test site explosions recorded on Lawrence Livermore National Laboratory's digital seismic system*, Bull. Seism. Soc. Am., *78*, 1759-1772.

PATTON, H.J., (2001), *Regional magnitude scaling, transportability, and* M_s:m_b *discrimination at small magnitudes*, Pure Appl. Geophys., *158*, 1951-2015.

PATTON, H.J., and SCHLITTENHARDT, J., (2005), *A transportability* $m_b(Lg)$ *scale for central Europe and implications for low-magnitude* M_s-m_b *discrimination*, Geophys. J. Int., *163*, 126-140.

PHILLIPS, W.S., and STEAD, R.J., (2008), *Attenuation of Lg in the western US using the USArray*, Geophys. Res. Lett., *35*, L07307, doi:10.1029/2007GL032926.

PRIESTLEY, K.F., and PATTON, H.J., (1997), *Calibration of* $m_b(Pn)$, $m_b(Lg)$ *scale and transportability of the* M_0:m_b *discriminant to new tectonic regions*, Bull. Seism. Soc. Am., *87* (5), 1083-1099.

RINGDAL, F., MARSHALL, P.D., and ALEWINE, R.W., (1992), *Seismic yield determination of Soviet underground explosions at the Shagan River test site*, Geophys. J. Int., *109*, 65-77.

SATO, T., SATO, T., SHINOHARA, M., HINO, R., NISHINO, and M., KANAZAWA, T., (2006), *P-wave velocity structure of the margin of the southeastern Tsushima Basin in the Japan Sea using ocean bottom seismometers and airguns*, Tectonophysics, *412*, 159-171.

SHI, J., RICHARDS, P.G. and KIM, W.-Y., (2000), *Determination of Seismic Energy from Lg Waves*, Bull. Seism. Soc. Am., *90* (2), 483-493.

VERGINO, E.S., and MENSING, R.W., (1990), *Yield estimation using regional* $m_b(Pn)$, Bull. Seism. Soc. Am., *80* (3), 656-674.

XIE, J., WU, Z., LIU, R., SCHAFF, D., LIU, Y., and LIANG, J., (2006), *Tomographic regionalization of crustal Lg Q in eastern Eurasia*, Geophys. Res. Lett., 33, L03315, doi:10.1029/2005GL024410.

YANG, X., (2002), *A numerical investigation of Lg geometrical spreading*, Bull. Seism. Soc. Am., *92* (8), 3067-3079.

ZHANG, T.-R., and LAY, T., (1995), *Why the Lg phase does not traverse oceanic crust*, Bull. Seism. Soc. Am., *85* (6), 1665-1678.

ZHAO, L.-F., XIE, X.-B., WANG, W.-M., and LAY, T., (2008), *Regional seismic characteristics of the 9 October 2006 North Korean Nuclear Test*, Bull. Seism. Soc. Am., *98* (6), 2571-2589.

(Received December 7, 2010, revised April 17, 2011, accepted April 18, 2011, Published online May 25, 2011)